2018

# Heat Transfer Process Within The R744 Two-phase Ejector: Numerical And Experimental Study

Michal Haida
*Silesian University of Technology, Poland*, Michal.Haida@polsl.pl

Jacek Smolka
*Silesian University of Technology, Poland*, jacek.smolka@polsl.pl

Armin Hafner
*NTNU Trondheim, Norway*, armin.hafner@ntnu.no

Mikolaj Mastrowski
*Silesian University of Technology, Poland*, mikolaj.mastrowski@gmail.com

Michal Palacz
*Silesian University of Technology, Poland*, michal.palacz@polsl.pl

***See next page for additional authors***

**Authors**
Michal Haida, Jacek Smolka, Armin Hafner, Mikolaj Mastrowski, Michal Palacz, Kenneth B. Madsen, Andrzej J. Nowak, and Krzysztof Banasiak

# Heat transfer process within the R744 two-phase ejector: numerical and experimental study

Michal HAIDA[1]*, Jacek SMOLKA[1], Armin HAFNER[2], Mikolaj MASTROWSKI[1], Michal PALACZ[1], Kenneth B. MADSEN[3], Andrzej J. NOWAK[1], Krzysztof BANASIAK[4]

[1]Silesian University of Technology, Institute of Thermal Technology,
Gliwice, Poland
Tel. +48322372810, fax. +48322372872, michal.haida@polsl.pl

[2]NTNU, Department of Energy and Process Engineering,
Trondheim, Norway
armin.hafner@ntnu.no

[2] Danfoss A/S,
Nordborg, Denmark
kbm@danfoss.com

[2] SINTEF Energy Research,
Trondheim, Norway
krzysztof.banasiak@sintef.no

* Corresponding Author

## ABSTRACT

The proposed three dimensional CFD model to simulate the influence of the heat transfer on the R744 two-phase ejector performance is presented. The numerical model was developed based on the homogeneous real fluid flow assumption with the enthalpy-based formulation of the energy equation. The R744 two-phase ejector was designed to evaluate the temperature profile within the ejector walls. The prototype R744 ejector for experimental investigation was manufactured by Institute of Thermal Technology and ATM in Poland. The performance measurements were carried out at a R744 test facility at SINTEF/NTNU in Norway. The foregoing ejector was equipped with the thirteen thermocouples located inside the ejector to measure the wall temperature in different ejector section i.e. the motive nozzle, the suction nozzle, the mixing section and the diffuser. The experimental test campaign at different operating conditions typical for refrigeration application was carried out and the uncertainty of the measurement was defined. Moreover, the experimental data are applied to validate the CFD results at defined operating conditions. The numerical results were set to evaluate the influence of the wall temperature on the two-phase flow parameters. In addition, the heat transfer coefficient of the two-phase flow within the ejector was estimated. The analysis of the heat transfer process within the R744 two-phase ejector let to investigate the influence of the ambient conditions and the different temperature levels of the motive and suction streams on the ejector performance.

## 1. INTRODUCTION

The recent legislation regulations of the European Union and the declarations presented during COP21 conference in Paris forces the industry to replace the common synthetic refrigerant i.e. hydro-fluorocarbons (HFCs) with more environmentally friendly synthetic refrigerants or/and preferably natural working fluids (Parliament & Council of the European Union, 2014). The preferred working fluid in new commercial refrigeration systems is carbon dioxide (denoted as R744) due to its non-flammability, non-toxicity and the satisfactory thermal properties (Kim, Pettersen, & Bullard, 2004). The modern $CO_2$-based refrigeration systems were first introduced in the Scandinavian region and in the northern and central part of United States of America (Hafner, Forsterling, & Banasiak, 2014; Sharma, Fricke, & Bansal, 2014). The modification of the R744 refrigeration system configuration let to utilise R744 refrigeration technology in hot climates at competitive energy performance when compared to the HFC-based systems (Gullo, Tsamos, Hafner, Ge, & Tassou, 2017). One of the solution to improve the system coefficient of performance (COP) is to introduce the two-phase ejector as the main expansion device (Elbel & Hrnjak, 2008).

The main aim of the ejector is to entrain the low-pressure suction stream by the supersonic expanded high-pressure motive stream and transferred the kinetic energy of the mixed flow into the pressure energy. Hence, the outlet pressure of the mixed stream is higher than the suction pressure. The integration of the two-phase ejector into the R744 refrigeration system improved the system energy performance when compared to the reference standard R744 direct expansion system up to 18% (Elbel, 2011). The theoretical and experimental investigations indicated high potential to improve the energy performance of the R744 refrigeration system equipped with the two-phase ejector. However, the ejector has to be design based on the complex mathematical model to work at high efficiency due to the phenomena complexity occurred inside the two-phase ejector (Besagni, Mereu, & Inzoli, 2016).

The more advanced numerical model of the two-phase ejector let to investigate the influence of the ambient conditions and the ejector shape design on the two-phase flow and the ejector performance at different operating conditions. Therefore, the coupling solution of the heat transfer process within the walls together with the $CO_2$ two-phase flow modelling is required. The two-phase flow inside the ejector can be modelled based on the computational fluid dynamics (CFD). The CFD model of the R744 ejector based on a homogeneous equilibrium model (HEM) was presented by Lucas et al. (2014) and Smolka et al. (2013a). In the work of Lucas et al. (2014), the numerical model was implemented in OpenFOAM open-source software and the investigation was done with and without the suction flow. The authors stated that the proposed model predicted the motive nozzle mass flux and the pressure recovery within an error margin of 10% without the suction flow and the discrepancy of the pressure recovery increased up to 20% when the suction flow was considered in the investigation.

Smolka et al. (2013a) developed the three-dimensional CFD enthalpy-based energy formulation model of the two-phase ejector. The authors implemented an enthalpy-based form and real fluid properties from the REFPROP libraries (Lemmon, Huber, & McLinden, 2010) for simulating carbon dioxide supersonic two-phase flow. The application range of HEM for the transcritical $CO_2$ two-phase ejector at typical supermarket conditions was presented by Palacz et al. (2015). The authors stated that the motive nozzle and the suction nozzle mass flow rate accuracies within ±10% was obtained for the motive nozzle conditions close and above the critical point. The numerical investigations performed by use of the HEM CFD model of the two-phase ejector let to simulate the real two-phase flow behaviour for the transcritical conditions with high accuracy. Although, the analysis of the R744 two-phase ejector in the subcritical region required more advanced numerical model. Palacz et al. (2017) compared the homogeneous relaxation model (HRM) with HEM to indicate the accuracy improvement for the operating conditions below the critical point. The authors implemented an additional vapour mass balance equation based on the numerical approach presented by Bilicki and Kestin et al. (1990). In addition, the relaxation time was defined according to the definition proposed by Angielczyk et al. (2010) for the $CO_2$ transcritical flow. The authors stated that the motive nozzle and the suction nozzle mass flow rate accuracies of HRM was higher than HEM for the subcritical region and the discrepancy of HRM increased in the transcritical region. Haida et al. (2017) presented the modified HRM of the two-phase flow inside the ejector. The authors implemented the modifications of the constant relaxation time coefficients to improve the model accuracy. The results of the R744 modified HRM two-phase flow inside the ejector confirmed that the application range of the modified HRM for the operating conditions typical for supermarket application extended compared to HEM for the motive nozzle pressure up to 60 bar.

Apart from the numerical investigation of the homogeneous fluid flow assumptions, the influence of the friction loss and the wall temperature on the supersonic ejector performance was analysed. Milazzo et al. (2017a) presented the influence of the different constant wall temperature and roughness on the R245fa ejector performance. The authors performed the numerical simulations close to the critical point of the two-dimensional axisymmetric CFD ejector model. The change of the constant wall temperature resulted in the different mass entrainment ratio. Moreover, the heat transfer coefficient (HTC) along the axis at the ejector wall was presented in (2017a). The authors stated that the heat loss toward the ambient should be considered for a precise sizing of the condenser and the ejector surfaces cannot be considered as adiabatic.

The main aim of this paper is to investigate the heat transfer process within the $CO_2$ two-phase ejector. To the best knowledge of the authors there is no such analysis in the literature. Hence, the numerical simulations were done including the non-adiabatic inner walls and the insulated outer walls. The $CO_2$ two-phase flows within the ejector was simulated based on the modified HRM proposed by Haida et al. (2017). The R744 prototype ejector was designed and manufactured for experimental investigation of the wall temperatures. The experimental test campaign on the $CO_2$ ejector test rig was carried out to validate the CFD model results at the NTNU/SINTEF Energy Research laboratory in Trondheim, Norway. Moreover, the heat transfer coefficient of the motive stream was presented in this paper.

## 2. The R744 ejector assembly

Figure 1 presents the R744 prototype ejector designed and manufactured to measure the wall temperature close to inner surfaces of the ejector. The ejector was assembled with three parts: the motive nozzle, the suction nozzle together with the mixer and the diffuser with the outlet port. A stainless steel was used to manufacture the motive nozzle part and a brass for the rest parts. The prototype ejector was assembled by bolting of eight screws. Standard type connectors were used to connect both inlet and outlet ports with a pipelines of a test rig. In addition, the thirteen small holes were drilled to insert the thermocouples for the wall temperature measurements of the investigated ejector.

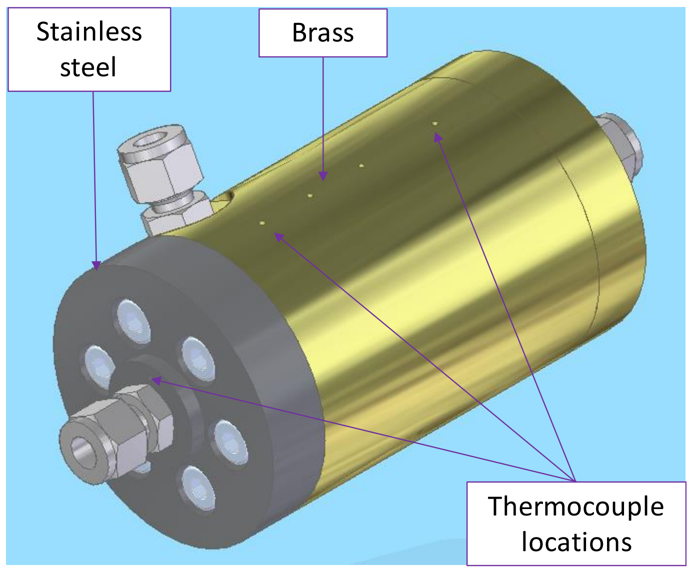


**Figure 1:** The R744 two-phase ejector assembly

The location of the temperature probes was shown in Figure 2. The position of the sensors was set to avoid the influence of the nearest thermocouple on the single measurement. The thermocouples were located to measure the wall temperature in the motive inlet, suction inlet, between the converging-diverging nozzle and the converging suction nozzle, the pre-mixer, the mixer and the diffuser. The distance between the inner wall surface and the probes was set to 2 mm. The main geometry parameters of the prototype ejector were listed in Table 1.

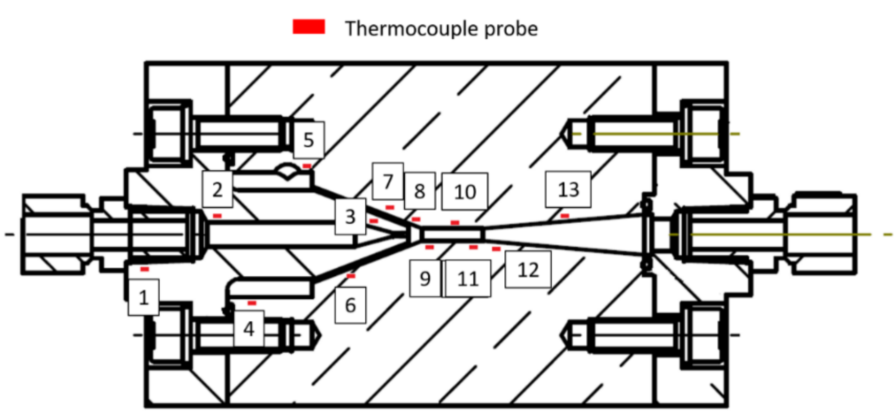

**Figure 2:** The thermocouple probe locations inside the prototype ejector

The designed and manufactured R744 prototype ejector allows for the experimental investigation of the wall temperature profile at different operating and ambient conditions. Therefore, the CFD model was developed to perform the simulations of the heat transfer in the prototype ejector and investigate the influence of the non-adiabatic walls on the ejector performance.

**Table1:** Main geometry parameter of the R744 prototype ejector

| Parameters | Unit | Geometry |
|---|---|---|
| Motive nozzle inlet diameter | mm | 6.0 |
| Motive nozzle throat diameter | mm | 0.9 |
| Motive nozzle outlet diameter | mm | 1.09 |
| Motive nozzle converging angle | ° | 30 |
| Motive nozzle diverging angle | ° | 2.0 |
| Diffuser outlet diameter | mm | 8.0 |
| Diffuser angle | ° | 5.0 |

## 3. The numerical approach

The proposed numerical model of the R744 two-phase ejector simulated the two-phase supersonic flow behaviour together with the heat transfer process occurred between the fluid flow and the ejector walls. In addition, the different ambient conditions were considered in the proposed model. The CFD model approach together with the computational procedure was described. In addition, the influence of the numerical mesh grid on the global and local parameters was presented.

The homogeneous relaxation flow assumption simplifies the numerical model to the mass, momentum, energy and vapour mass balance governing equations of the relaxation mixture. In addition, steady-state computations were performed for each operating condition. Therefore, all the time derivatives in the governing equations were omitted. The mass balance is described as follows:

$$\nabla \cdot (\bar{\rho}\tilde{\boldsymbol{u}}) = 0 \tag{1}$$

where the symbols ( $\bar{}$ ) and ( $\tilde{}$ ) denote the Reynolds- and Favre-averaged quantities, respectively. In addition, $\rho$ is the fluid density in kg/m$^3$ and **u** is the fluid velocity vector in m/s. The momentum balance is defined by the following equation:

$$\nabla \cdot (\bar{\rho}\tilde{\boldsymbol{u}}\tilde{\boldsymbol{u}}) = -\nabla\bar{p} + \nabla \cdot (\tilde{\boldsymbol{\tau}} + \boldsymbol{\tau}_T) \tag{2}$$

where $p$ is the pressure of the mixture fluid in Pa and $\tau$ is the stress tensor in N/m$^2$. The vapour mass balance equation is described in the following form (Bilicki & Kestin, 1990):

$$\nabla \cdot (\bar{\rho}\tilde{x}) = -\bar{\rho}\left(\frac{\tilde{x} - \tilde{x}_{eq}}{\tilde{\theta}}\right) \tag{3}$$

where $x$ is the instantaneous vapour quality of the two-phase flow, $x_{eq}$ is the vapour quality at the equilibrium state and $\theta$ is the relaxation time in s. According to Haida et al. (2017) the relaxation time for $CO_2$ two-phase flow is defined by the following equation:

$$\tilde{\theta} = \theta_0 \cdot \tilde{\alpha}^a \cdot \bar{\phi}^b \begin{cases} \theta_0 = 1.0e-07 \quad a = 0.0 \quad b = 0.0 & p_{mn} > 73.77\ bar \\ \theta_0 = 9.0e-06 \quad a = -0.67 \quad b = -1.73 & p_{mn} \in \langle 59\ bar; 73.77\ bar \rangle \\ \theta_0 = 1.5e-06 \quad a = -0.67 \quad b = -2.00 & p_{mn} < 59\ bar \end{cases} \tag{4}$$

where $\theta_0$, $a$ and $b$ are the constant relaxation time coefficients defined for different motive nozzle pressure ranges $p_{mn}$, $\alpha$ is the void fraction and $\phi$ is the non-dimensional pressure difference defined as follows:

$$\tilde{\alpha} = \frac{\tilde{x} \cdot \bar{\rho}}{\bar{\rho}_{sv}} \tag{5}$$

$$\bar{\varphi} = \left|\frac{\bar{p}_{sat} - \bar{p}}{p_{crit} - \bar{p}_{sat}}\right| \tag{6}$$

where $\rho_v$ is the density of the saturated vapour, $p_{sat}$ is the saturation pressure based on the motive nozzle inlet conditions and $p_{crit}$ is the critical pressure of $CO_2$. According to Smolka et al. (2013a), the temperature-based form of the energy equation can be replaced by the enthalpy-based form. Hence, the energy balance can be defined as follows:

$$\nabla \cdot \left(\bar{\rho}\tilde{\boldsymbol{u}}\tilde{E}\right) = \nabla \cdot \left[\left(\frac{k}{\frac{\partial h}{\partial T}}\right)_p \nabla\tilde{h} - \left(\frac{k}{\frac{\partial h}{\partial T}}\right)_p \left(\frac{\partial h}{\partial p}\right)_T \nabla\bar{p} + \tilde{\boldsymbol{\tau}} \cdot \tilde{\boldsymbol{u}}\right] \tag{7}$$

where $T$ is the mixture temperature in K, $k$ is the thermal conductivity of the fluid in W/(m·K) and $E$ is the total specific enthalpy defined as a sum of the specific mixture enthalpy and the kinetic energy:

$$\tilde{E} = \tilde{h} + \frac{\tilde{u}^2}{2} \tag{8}$$

where $h$ is the mixture specific enthalpy in J/(kg·K). The enthalpy-based form of the energy equation let to define fluid properties as a function of the pressure and specific enthalpy. The heat transfer in the ejector walls was simulated using heat conduction equation in the following equation:

$$\nabla(k_i \cdot \nabla T) = 0 \tag{9}$$

where $k_i$ is the thermal conductivity of the solid ejector walls in W/(m·K). The foregoing heat conduction equation was implemented using user-defined scalar (UDS) in Ansys Fluent software. The conjugate heat transfer method was used to couple heat transfer together with the two-phase flow based on the fourth kind boundary conditions. Hence, the developed model allowed continuity of temperature and heat flux at the interface between the fluid and the solid subdomains. Finally, the coupled mathematical model of the two-phase flow together with the non-adiabatic ejector walls was defined. The numerical approach was implemented to the discretised domain of the R744 two-phase ejector to perform the numerical computations at specified operating conditions, heat transfer wall conditions and ambient conditions.

The partial differential equations of the mathematical model were solved based on the PRESTO scheme for the pressure discretisation and the second-order upwind scheme for the other variables considered in the CFD model. The coupled method was employed for the coupling of the pressure and velocity fields. The k-$\varepsilon$ Realisable model was used to model the turbulent flow inside the ejector (Fluent, 2011). The real fluid properties of R744 were approximated based on data obtained using the REFPROP libraries (Lemmon et al., 2010).

The 3-D prototype ejector geometry was discretised with a fully structured grid as shown in Figure 3. The numerical grid considered three domains regarding the two-phase flow and two ejector walls with different material. The wall roughness was set to 2 μm according to the ejectors manufacturers. The ejector mesh independence study was done to avoid the influence of the mesh grid on the ejector performance and the mesh with 1.3 million elements was selected to the validation procedure and the further numerical investigations. In addition, the chosen mesh grid obtained the minimum orthogonal quality above 0.6.

The CFD computations were done by use of the pressure-based boundary conditions of the fluid. The outer walls of the prototype ejector were isolated, thereby the zero heat flux boundary condition was assumed in each outer wall. The inner walls were defined either as the adiabatic wall or the non-adiabatic wall. The adiabatic boundary condition of the inner walls does not consider the heat transfer between the $CO_2$ stream and the inner walls of the each ejector part. The influence of the heat transfer on the R744 two-phase flow behaviour can be taken into account by assuming of the non-adiabatic inner walls boundary conditions. Hence, the validation procedure of the proposed CFD model let to define the accuracy of the model by the evaluation of the motive nozzle and suction nozzle mass flow rates (MFR) predictions as well as the prediction of the ejector wall temperatures.

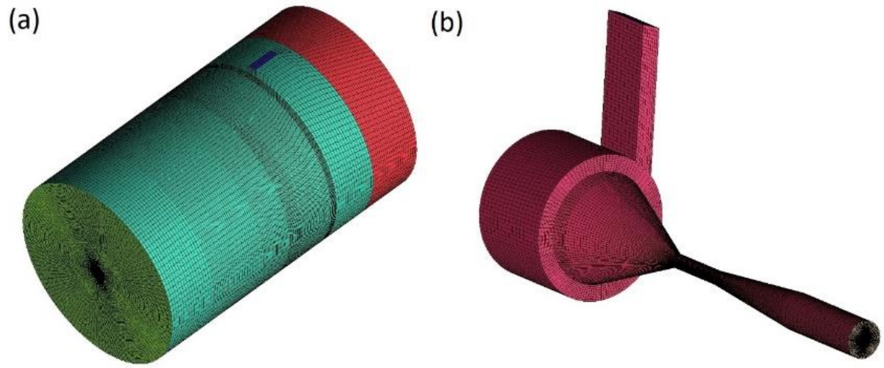


**Figure 3:** The numerical mesh grid of the R744 prototype ejector: (a) steel and brass domains; (b) $CO_2$ domain

## 4. R744 vapour compression test rig equipped with the prototype ejector

The designed and manufactured R744 prototype ejector was integrated into an entire refrigeration loop, applying the experimental test facility at the NTNU/SINTEF laboratories in Trondheim, Norway. In addition, the pressure test was accomplished to locate any leakage inside the ejector before it was connected to the system. The test rig is the R744 vapour compression rack fully equipped with the measurement sensors to carry out the experimental investigation of the expansion devices, i.e. the capillary tube or the ejector. Figure 4 presents the integration of the R744 prototype ejector together with the $CO_2$ system before the ejector coverage by a thermal insulation. Moreover, the pressure and temperature sensors of the nozzles and outlet collectors were shown.

The test facility is fully equipped with pressure, temperature and the mass flow rate sensors, for which the accuracies were taken from product data-sheet. The temperature was measured in the nozzles and outlet collectors by the resistance thermometers PT100 class A with the accuracy of ±(0.15 + 0.002 *T*), where *T* is the temperature in °C. The wall measurements were done by use of the T-type calibrated thermocouples with the accuracy of ±0.75% of reading. The piezoelectric transmitter was used to measure the pressure with the accuracy of ±0.3% of reading. The MFR measurement was done by use of the Coriolis type RHM04 and RHM06 transducers and the accuracy was of ±0.2% of reading. The output signals from sensors installed in the test rig were processed and transmitted by the National Instruments control unit to the LabView system. The data were exported as a CSV standard to the uncertainty analysis. The test campaign was carried out to obtain the transcritical and close to critical point operating conditions of the motive nozzle for a set of temperature differences between the motive nozzle and the suction nozzle.

$$\Delta T = T_{mn} - T_{sn} \tag{10}$$

The steady state conditions of the experimental single point were defined as a stable parameters of the nozzles and outlet collectors as well as the mass flow rates and the ejector wall temperatures in the period of ten minutes. Hence, the validation procedure of the proposed CFD model was done for different motive nozzle, suction nozzle and pressure operating conditions. The selected operating conditions (OC) to the validation procedure were set in Table 2.

**Table2:** Operating conditions of the R744 prototype ejector for validation procedure

| OC | $P_{mn}$ | $T_{mn}$ | $P_{sn}$ | $T_{sn}$ | $P_{out}$ | ΔT |
|---|---|---|---|---|---|---|
| | bar | K | bar | K | bar | K |
| #1 | 87.4 | 294.8 | 38.8 | 283.2 | 39.5 | 11.5 |
| #2 | 106.3 | 306.9 | 36.6 | 280.5 | 39.0 | 26.4 |

The accuracy of the selected parameter of the numerical model was calculated as the relative error between the experimental (exp) and the numerical results (num) of the motive nozzle MFR or the suction nozzle MFR.

$$\delta_{\dot{m}} = \frac{\dot{m}_{num} - \dot{m}_{exp}}{\dot{m}_{exp}} \cdot 100\% \tag{11}$$

where $\delta_{\dot{m}}$ is the relative error, $\dot{m}$ is the motive nozzle MFR or the suction nozzle MFR given by the experimental data or the numerical results. The acceptable relative difference between the experimental and the numerical results was assumed as less than or equal to 15% for the mass flow rates and less than or equal to 5% for the wall temperature measurements .

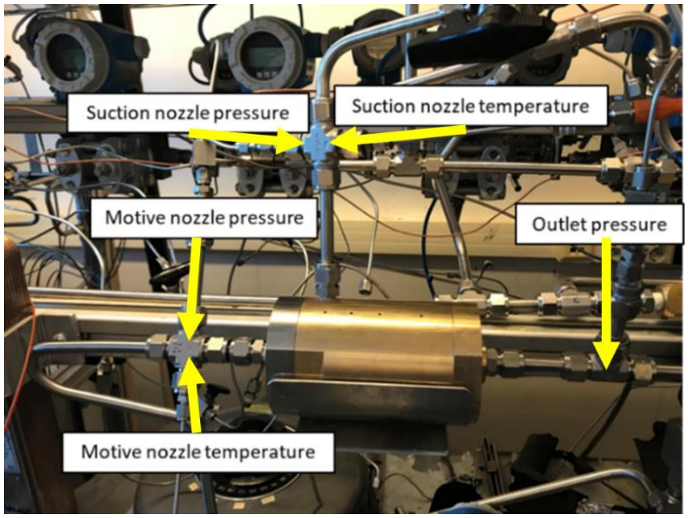


**Figure 4:** The integration of the R744 prototype ejector together with the vapour compression test rig and the ejector collectors measurements.

The performance of the $CO_2$ two-phase ejector can be defined by the mass entrainment ratio parameter, which is a ration between the suction nozzle MFR and the motive nozzle MFR:

$$MER = \frac{\dot{m}_{sn}}{\dot{m}_{mn}} \tag{12}$$

The heat transfer behaviour between the $CO_2$ two-phase flow and the ejector walls can be defined by the heat transfer coefficient (HTC). The evaluation of the heat transfer coefficient within the R744 ejector allowed the proper selection of the wall material and the consideration of the heat transfer into the ejector shape design process. The HTC was defined as follows:

$$HTC = \frac{q}{(|\mathrm{T}_{wall} - T_{stream}|)} \tag{13}$$

where *HTC* is the heat transfer coefficient in $W/(m^2 \cdot K)$ and $q$ is the heat flux in $W/m^2$. The temperature $\mathrm{T}_{wall}$ is the local wall temperature and $T_{stream}$ is the near wall fluid temperature.

## 5. Results

The results of the validation procedure were set in Table 3. The accuracies of the motive nozzle and the suction nozzle MFRs together with all ejector wall temperature probes for two different operating conditions were presented. The discrepancy of the motive nozzle MFR was within ±3% for both operating conditions. In addition, the suction nozzle MFR given by the CFD model was higher than from the experimental data of approximately 15%. The accuracy of each wall temperature was within ±2%. Hence, the proposed CFD model obtained high accuracy of the wall temperature prediction at acceptable range of the motive nozzle and the suction nozzle MFRs. The high accuracy of the developed CFD model confirmed that the integration of the modified HRM model of the $CO_2$ two-phase flow together with the heat transfer process allows detailed investigation of the ejector shape influence on the ejector performance.

**Table3:** The mass flow rates and wall temperatures accuracies of the proposed CFD model

| Relative error, % | | | | | | | | | | | | | | |
|---|---|---|---|---|---|---|---|---|---|---|---|---|---|---|
| OC | $MFR_{MN}$ | $MFR_{SN}$ | $T_1$ | $T_2$ | $T_3$ | $T_4$ | $T_5$ | $T_6$ | $T_7$ | $T_8$ | $T_9$ | $T_{10}$ | $T_{11}$ | $T_{12}$ | $T_{13}$ |
| 1 | -2.3 | 14.9 | 0.6 | 0.7 | 0.1 | 0.7 | 0.9 | 0.9 | 0.9 | 1.4 | 1.2 | 1.6 | 1.4 | 0.7 | -0.1 |
| 2 | 2.5 | -8.5 | 2.6 | 0.3 | -4.0 | 1.3 | 1.5 | 1.6 | 2.8 | 2.0 | 2.7 | 2.1 | 3.4 | 0.5 | -0.1 |

Figure 5 presents the temperature field and the mass entrainment ratio of the $CO_2$ prototype ejector for the adiabatic and non-adiabatic inner walls of the ejector. The temperature field of the ejector with the adiabatic wall presented in Figure 5a was defined only for $CO_2$ two-phase flow inside the ejector as the ejector walls were defined as the insulated wall. It can be seen that the consideration of the wall temperature influenced on the temperature of the $CO_2$ flow, especially in the diverging part of the motive nozzle and in the mixing chamber. Moreover, the prototype ejector with the non-adiabatic wall obtained lower mass entrainment ratio when compared to the case with the adiabatic walls.

Hence, the proper selection of the ejector wall material with a low value of the thermal conductivity could reduce the influence of the heat transfer on the degradation of the ejector performance.

Figure 6 presents the HTC along the motive nozzle of the R744 prototype ejector at the boundary conditions #1 defined in Table 2. The motive nozzle wall selected for HTC calculations was presented in Figure 5(b). The HTC was in the range from 5000 W/(m$^2$·K) to approximately 37000 W/(m$^2$·K). It can be seen that the HTC significantly increased during the stream expansion in the converging-diverging nozzle. Moreover, the lowest HTC was obtained before the converging part, where the stream temperature was similar to the motive nozzle temperature, but the wall temperature decreased. The highest HTC was obtained at the end of the motive nozzle as the result of the smallest distance between the both streams and the influence of the low suction stream temperature on the wall temperature. Therefore, the high HTC of the motive stream influenced on the ejector performance as the $CO_2$ flow temperature decreased close to the inner walls.

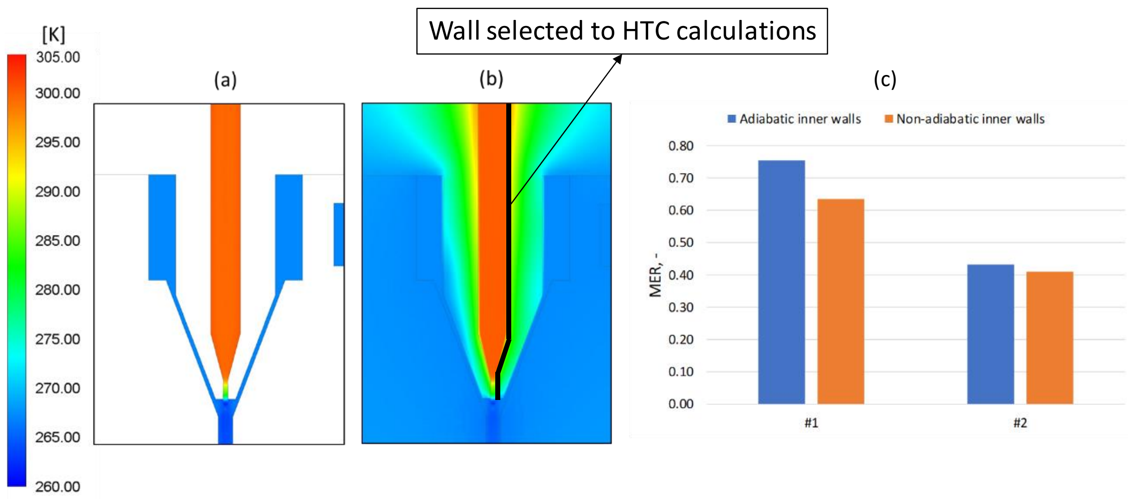


**Figure 5:** Temperature field in K of the $CO_2$ prototype ejector at OC #1 defined in Table 2: (a) adiabatic inner walls; (b) non-adiabatic inner walls; (c) mass entrainment ratio at OCs #1 and #2

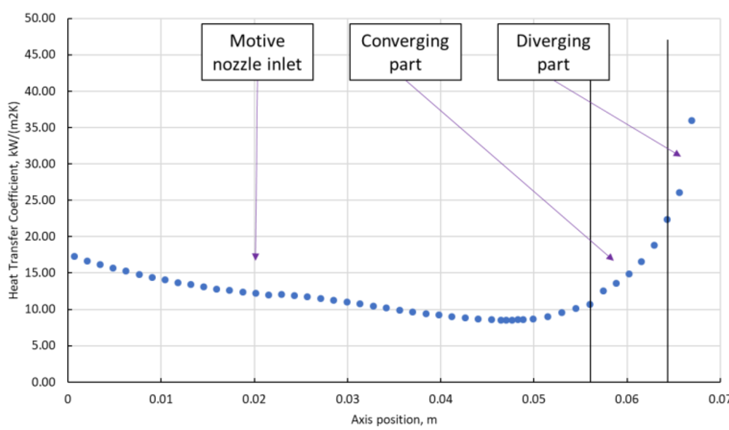


**Figure 6:** Heat transfer coefficient in kW/(m$^2$·K) of the $CO_2$ two phase flow along the motive nozzle at OC#1 defined in Table 2

## 6. Conclusions

The proposed CFD model of the $CO_2$ two phase ejector was developed by coupling the modified HRM two-phase flow assumption together with the heat transfer within the ejector walls. The developed three-dimensional model was verified and validated to define the accuracy of the CFD model. The mesh sensitivity analysis was carried out to avoid the influence of the numerical mesh grid on the ejector performance. The validation procedure of the developed CFD model confirmed a good prediction of the mass flow rates. The motive nozzle MFR accuracy was within ±5% and the suction nozzle MFR accuracy was within ±15%. Moreover, the wall temperatures prediction of the prototype R744 ejector CFD model was within ±2%. Therefore, the developed CFD model let to investigate the influence of the heat transfer on the ejector performance and calculated the HTC of the $CO_2$ two-phase flow.

The non-adiabatic inner walls of the R744 prototype ejector decreased MER up to 15% and 11% at OC #1 and #2, respectively. Therefore, a use of the low thermal conductivity materials reduces the negative influence of the heat transfer on the ejector performance. However, the selection of the material to manufacture the ejector should also consider the stress analysis in the motive nozzle as the result of the expansion process to avoid any device breakdown. The HTC along the motive nozzle confirmed the influence of the heat transfer on the $CO_2$ two-phase flow, especially in the converging-diverging nozzle. The HTC calculations of the other ejector parts, i.e. suction nozzle, mixing chamber and diffuser will be presented during the conference.

## NOMENCLATURE

| | | |
|---|---|---|
| E | Total enthalpy | (kJ/kg) |
| h | Specific enthalpy | (kJ/kg) |
| HTC | Heat transfer coefficient | (W/(m$^2$/K) |
| k | Effective thermal conductivity | (W/m/K) |
| $\dot{m}$ | Mass flow rate | (kg/s) |
| p | Pressure | (bar) |
| T | Temperature | (K) |
| **u** | Velocity vector | (m/s) |
| q | Heat flux | (W/m$^2$) |
| x | Local vapour quality | (-) |
| α | Void fraction | (-) |
| φ | Non dimensional pressure difference | (-) |
| δ | Relative error | (%) |
| θ | Relaxation time | (s) |
| ρ | Density | (kg/m$^3$) |
| τ | Stress tensor | (N/m$^2$) |

**Subscript**

| | |
|---|---|
| crit | Critical conditions |
| exp | Experiment |
| mn | Motive nozzle |
| num | Numerical CFD model |
| sn | Suction nozzle |
| sat | Saturation conditions |
| v | Saturated vapour |

## REFERENCES

Angielczyk, W., Bartosiewicz, Y., Butrymowicz, D., & Seynhaeve, J.-M. (2010). Purdue e-Pubs 1-D Modeling Of Supersonic Carbon Dioxide Two-Phase Flow Through Ejector Motive Nozzle. Retrieved from http://docs.lib.purdue.edu/iracc

Banasiak, K., & Hafner, A. (2011). 1D Computational model of a two-phase R744 ejector for expansion work recovery. *International Journal of Thermal Sciences*, *50*(11), 2235–2247. https://doi.org/http://dx.doi.org/10.1016/j.ijthermalsci.2011.06.007

Besagni, G., Mereu, R., & Inzoli, F. (2016). Ejector refrigeration: A comprehensive review. *Renewable and Sustainable Energy Reviews*. https://doi.org/10.1016/j.rser.2015.08.059

Bilicki, Z., & Kestin, J. (1990). Physical Aspects of the Relaxation Model in Two-Phase Flow. *Proceedings of the Royal Society of London A: Mathematical, Physical and Engineering Sciences*, *428*(1875), 379–397. Retrieved from http://rspa.royalsocietypublishing.org/content/428/1875/379.abstract

Elbel, S. (2011). Historical and present developments of ejector refrigeration systems with emphasis on transcritical carbon dioxide air-conditioning applications. *International Journal of Refrigeration-Revue Internationale Du Froid*, *34*(7), 1545–1561. https://doi.org/DOI 10.1016/j.ijrefrig.2010.11.011

Elbel, S., & Hrnjak, P. (2008). Experimental validation of a prototype ejector designed to reduce throttling losses encountered in transcritical R744 system operation. *International Journal of Refrigeration-Revue Internationale Du Froid*, *31*(3), 411–422. https://doi.org/DOI 10.1016/j.ijrefrig.2007.07.013

Fluent, A. (2011). *Ansys Fluent User's Guide*. P.A. Canonsburg.

Gullo, P., Tsamos, K., Hafner, A., Ge, Y., & Tassou, S. A. (2017). State-of-the-art technologies for transcritical R744 refrigeration systems – a theoretical assessment of energy advantages for European food retail industry. *Energy Procedia*, *123*, 46–53. https://doi.org/https://doi.org/10.1016/j.egypro.2017.07.283

Hafner, A., Forsterling, S., & Banasiak, K. (2014). Multi-ejector concept for R-744 supermarket refrigeration. *International Journal of Refrigeration-Revue Internationale Du Froid*, *43*, 1–13. https://doi.org/DOI 10.1016/j.ijrefrig.2013.10.015

Haida, M., Smolka, J., Hafner, A., Palacz, M., Banasiak, K., & Nowak, A. J. (2017). Modified homogeneous relaxation model for the R744 trans-critical flow in a two-phase ejector. *International Journal of Refrigeration*. https://doi.org/10.1016/j.ijrefrig.2017.10.010

Kim, M. H., Pettersen, J., & Bullard, C. W. (2004). Fundamental process and system design issues in {CO}$_2$ vapor compression systems. *Progress in Energy and Combustion Science*, *30*(2), 119–174. https://doi.org/10.1016/j.pecs.2003.09.002

Lemmon, E. W., Huber, M. L., & McLinden, M. O. (2010). NIST Standard Reference Database 23: Reference Fluid Thermodynamic and Transport Properties - REFPROP. *National Institute of Standards and Technology, Standard Reference Data Program*.

Lucas, C., Rusche, H., Schroeder, A., & Koehler, J. (2014). Numerical investigation of a two-phase CO2 ejector. *International Journal of Refrigeration*. https://doi.org/10.1016/j.ijrefrig.2014.03.003

Milazzo, A., & Mazzelli, F. (2017). Future perspectives in ejector refrigeration. *Applied Thermal Engineering*, *121*, 344–350. https://doi.org/https://doi.org/10.1016/j.applthermaleng.2017.04.088

Palacz, M., Haida, M., Smolka, J., Nowak, A. J., Banasiak, K., & Hafner, A. (2017). HEM and HRM accuracy comparison for the simulation of CO2 expansion in two-phase ejectors for supermarket refrigeration systems. *Applied Thermal Engineering*, *115*, 160–169. https://doi.org/10.1016/j.applthermaleng.2016.12.122

Palacz, M., Smolka, J., Fic, A., Bulinski, Z., Nowak, A. J., Banasiak, K., & Hafner, A. (2015). Application range of the HEM approach for CO2 expansion inside two-phase ejectors for supermarket refrigeration systems. *International Journal of Refrigeration*, *59*, 251–258.

Parliament, E., & Council of the European Union. (2014). Regulation (EU) no. 517/2014 of the European Parliament and of the council on fluorinated greenhouse gases and repealing regulation (EC) no 842/2006 text with EEA relevance.

Sharma, V., Fricke, B., & Bansal, P. (2014). Comparative analysis of various CO2 configurations in supermarket refrigeration systems. *International Journal of Refrigeration-Revue Internationale Du Froid*, *46*, 86–99. https://doi.org/DOI 10.1016/j.ijrefrig.2014.07.001

Smolka, J., Bulinski, Z., Fic, A., Nowak, A. J., Banasiak, K., & Hafner, A. (2013). A computational model of a transcritical R744 ejector based on a homogeneous real fluid approach. *Applied Mathematical Modelling*, *37*(3), 1208–1224. https://doi.org/http://dx.doi.org/10.1016/j.apm.2012.03.044

## ACKNOWLEDGEMENT

The authors gratefully acknowledge the financial support of the Research Council of Norway through project No. 244009/E20. The work of MH was also partially supported by the Rector's research grant No. 08/060/RGJ18/0157 provided by SUT.